Supplementary Information: DNA Calorimetric Force Spectroscopy at Single Base Pair Resolution

P. Rissone[1,2], M. Rico-Pasto[3,4], S. B. Smith[5] and F. Ritort[1,6,7*]

[1]Small Biosystems Lab, Condensed Matter Physics Departement, Universitat de Barcelona, C/ Marti i Franques 1, Barcelona, 08028, Spain.
[2]Physics Departement, Sapienza University of Rome, Piazzale Aldo Moro 5, Rome, 00165, Italy.
[3]Unit of Biophysics and Bioengineering, Department of Biomedicine, School of Medicine and Health Sciences, Universitat de Barcelona, C/Casanoves 143, Barcelona, 08036, Spain.
[4]Institute for Bioengineering of Catalonia (IBEC), The Barcelona Institute for Science and Technology (BIST), Barcelona, 08028, Spain.
[5]Steven B. Smith Engineering, Los Lunas, New Mexico, USA.
[6]Reial Acadèmia de Ciències i Arts de Barcelona (RACAB), Secció Física.2a, La Rambla 115, Barcelona, E-08002, Spain.
[7]Institut de Nanociència i Nanotecnologia (IN2UB), Barcelona, Spain.

*Corresponding author(s). E-mail(s): ritort@ub.edu;
Contributing authors: rissone.paolo@gmail.com; m.rico.pasto@gmail.com; stevesmith@gmail.com;

Contents

Supplementary Figures

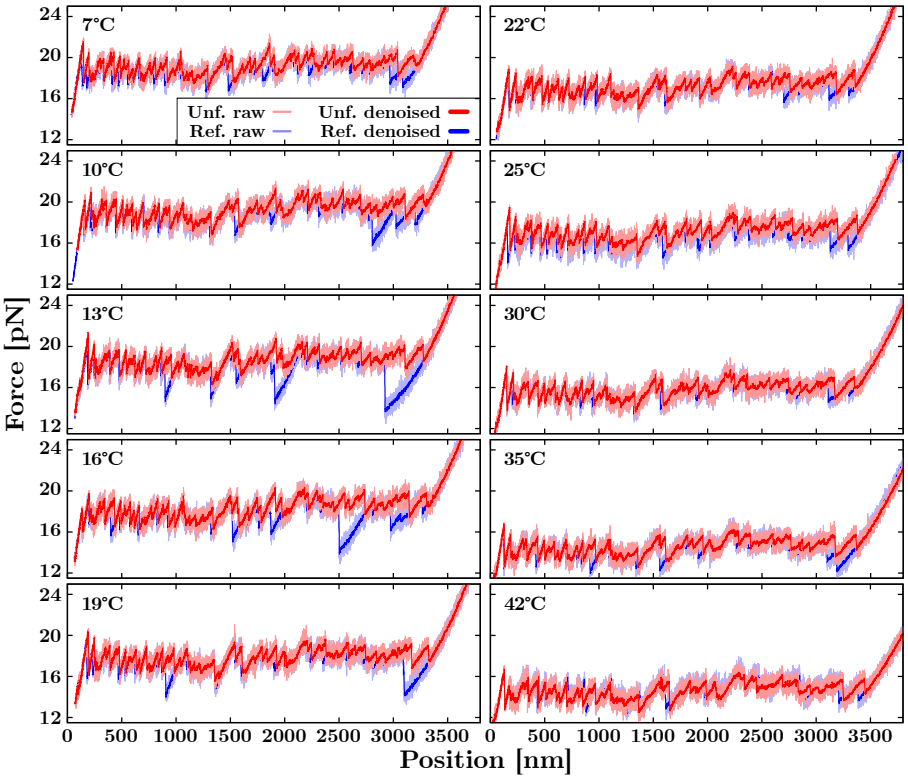

Supplementary Fig. 1: **Raw unzipping data.** Each panel shows one unfolding/refolding cycle for one molecule at a given T. Unzipping (red) and rezipping (blue) curves show a small hysteresis except for sporadic refolding events and particularly in correspondence of the first force jump observed during the refolding upon initiation of stem formation from the ssDNA. The light-colored lines are the raw data at 1kHz, while darker lines are raw data after denoising. This is done by applying a Savitzky–Golay filter over time windows of 150ms. Source data are provided as a Source Data file.

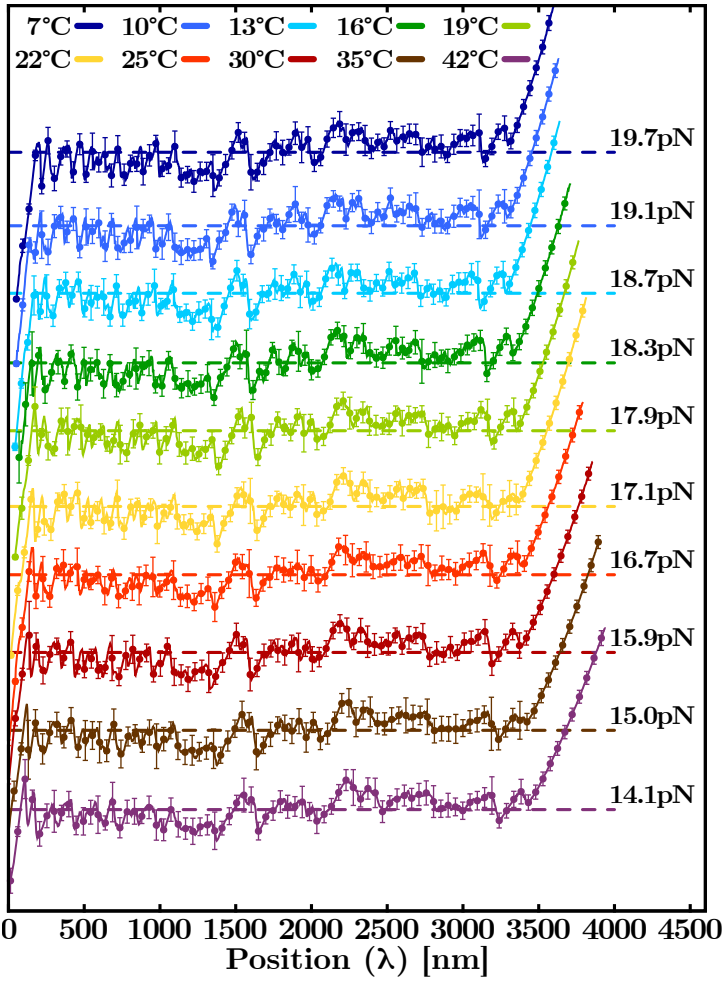

Supplementary Fig. 2: T**-dependent of the average FDCs.** At each T, the FDC results from averaging over 5−6 molecules for 40−50 unzipping/rezipping cycles. The error bars are the standard deviation in force (plotted for a fraction of the total data points) and show the molecule-to-molecule variability. The dashed lines show the average unzipping force at each temperature. Source data are provided as a Source Data file.

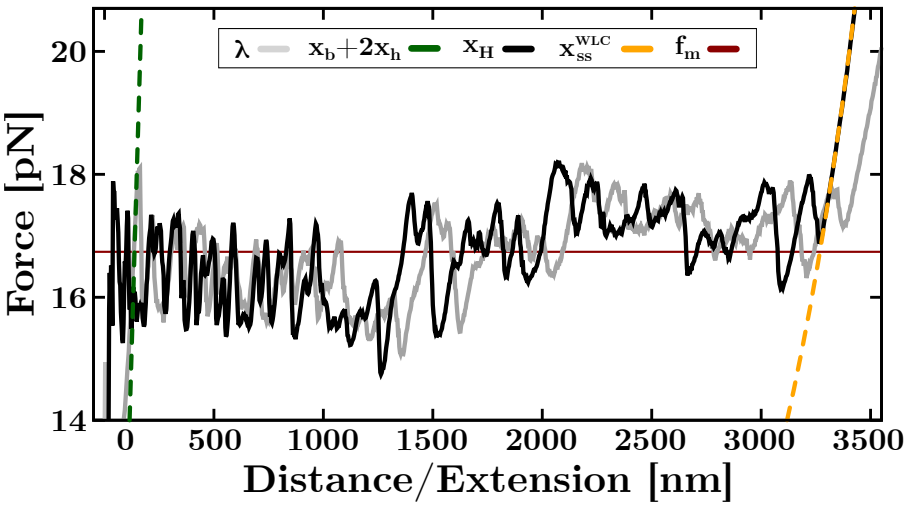

Supplementary Fig. 3: **Computation of the FEC from the experimental FDC**. The force versus hairpin extension, x_H, (black line) is computed by subtracting to the trap position, λ, (grey line) the elastic contribution of the optically trapped bead, x_b, and DNA handles, $2x_h$, (green dashed line). To measure the T-dependent ssDNA elasticity, we fit the FEC after the last rip to the WLC model (orange dashed line). Notice that the average unzipping force, f_m, (red line) remains constant upon computing the FEC. Data are shown at $T = 25°$C. Source data are provided as a Source Data file.

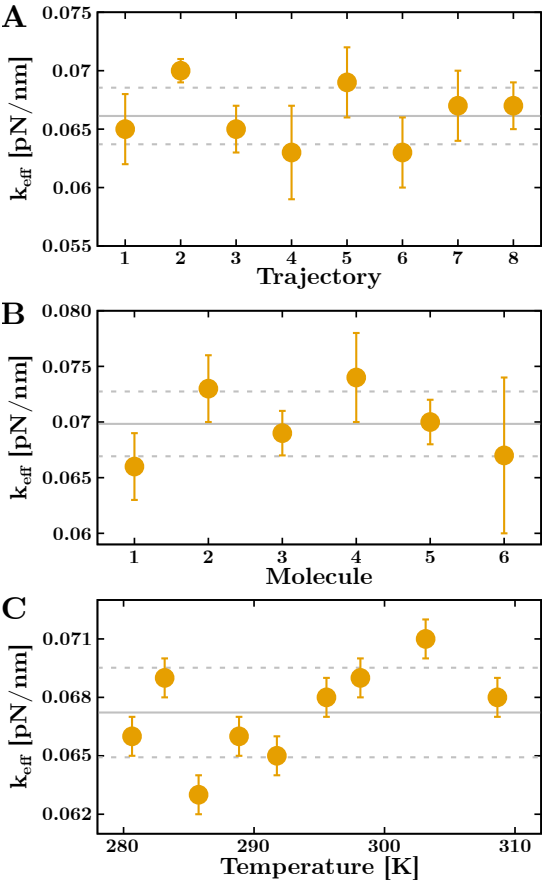

Supplementary Fig. 4: Experimental measurement of the effective stiffness. The effective stiffness, k_{eff}, has been obtained by fitting the first slope of the FDC between 3pN and the first rip to the linear equation $f = k_{\text{eff}}x$ (see Supplementary Methods, Sec. 2). Panels (**A**) and (**B**) show the k_{eff} variability among different trajectories (for one selected molecule) and molecules (after having averaged over cycles for each molecule) at 25°C. Panel (**C**) reports k_{eff} at each experimental temperature. The continuous line indicates the average value and the dashed lines show the corresponding error. All data are presented as mean values +/− SE. Source data are provided as a Source Data file.

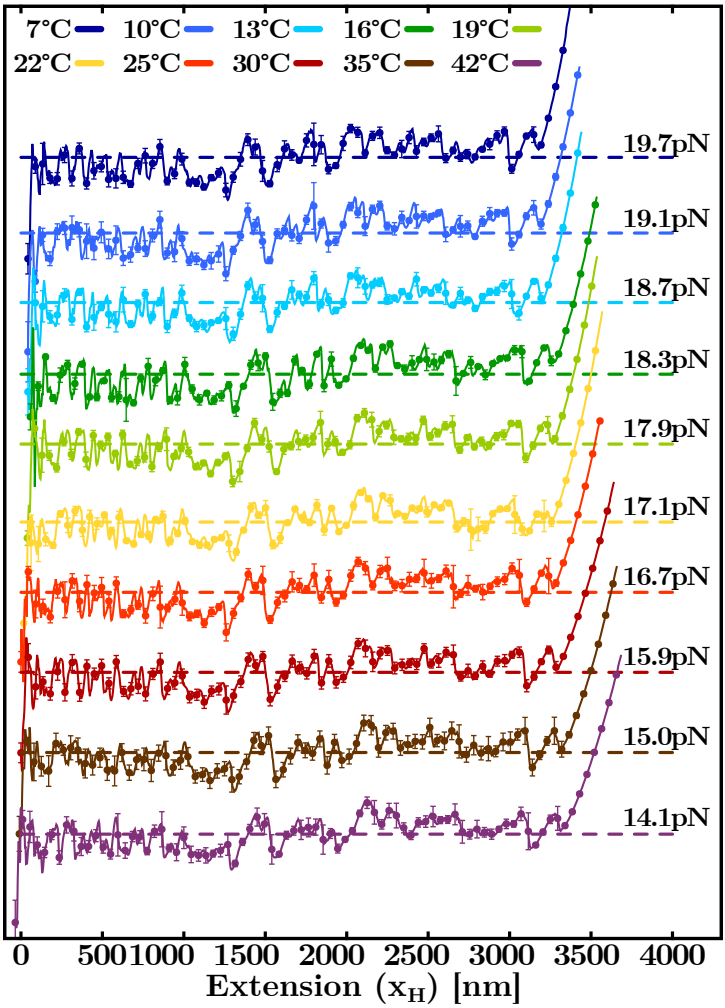

Supplementary Fig. 5: **Temperature dependence of the average force-extension curves (FECs) .** At each T, the FEC is obtained by subtracting the contributions of the optically trapped bead and the dsDNA handles ($x_\mathrm{b} + 2x_\mathrm{h}$) to the total trap-pipette distance λ (see main text). FECs are computed from the corresponding average FDCs. All data are presented as mean values +/− SE. Source data are provided as a Source Data file.

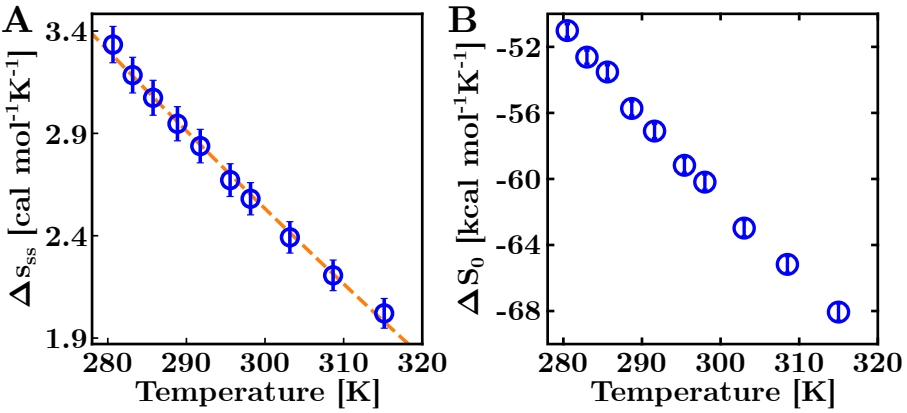

Supplementary Fig. 6: **Clausius-Clapeyron equation applied over the full FDC.** (**A**) T-dependence of the entropy change per base, Δs_{ss}. It accounts for the work to stretch the ssDNA and orient the folded molecule along the direction of the external force, from $f = 0$pN to $f_{\rm m}(T)$ (integral term in Eq.(2), main text). The results are reported in Supplementary Table 3. A fit to data according to $\Delta s_{\rm ss}(T) = \Delta s_{\rm ss,0} + \Delta c_p^{\rm ss} \log(T/T_m)$ (orange dashed line), gives the ssDNA heat capacity change per base at zero force, $\Delta c_p^{\rm ss} = -11.2 \pm 0.2\,{\rm cal\,mol^{-1}K^{-1}}$. (**B**) T-dependence of the total entropy change, $\Delta S_0(T)$, upon unzipping the 3.6kbp DNA hairpin measured using the Clausius-Clapeyron equation (see Eq.(2), main text). All data are presented as mean values +/− SE. Source data are provided as a Source Data file.

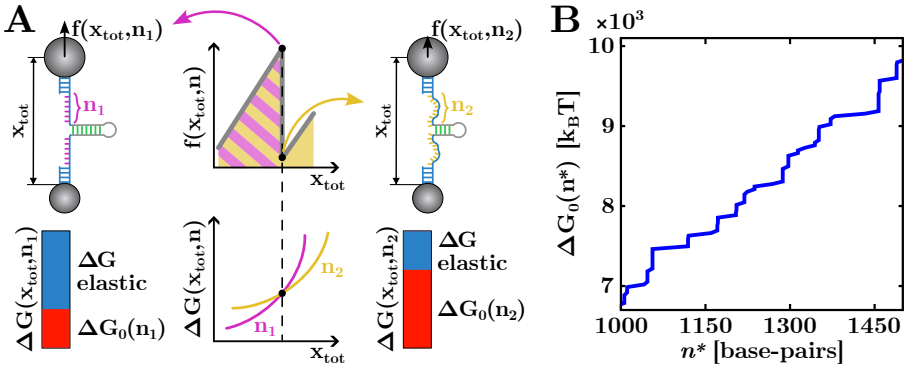

Supplementary Fig. 7: **Derivation of the theoretical FDC.** (**A**) Schematics of the stretching and hybridization energy contributions. Upon unzipping, the molecule has n_1 open bp before the force rip (left) and $n_2 > n_1$ open bp after the rip (right). At the force rip (black dots), the total free energy of the system is the same in both states, and the system changes from the highest free energy branch (n_1, pink) to the lowest energy branch (n_2, yellow). (**B**) The free energy of hybridization upon unzipping the hairpin is a monotonically increasing step function, with each discontinuity corresponding to a rip along the equilibrium FDC. Figure adapted from [1], available under the CC-BY-NC-ND license. Source data are provided as a Source Data file.

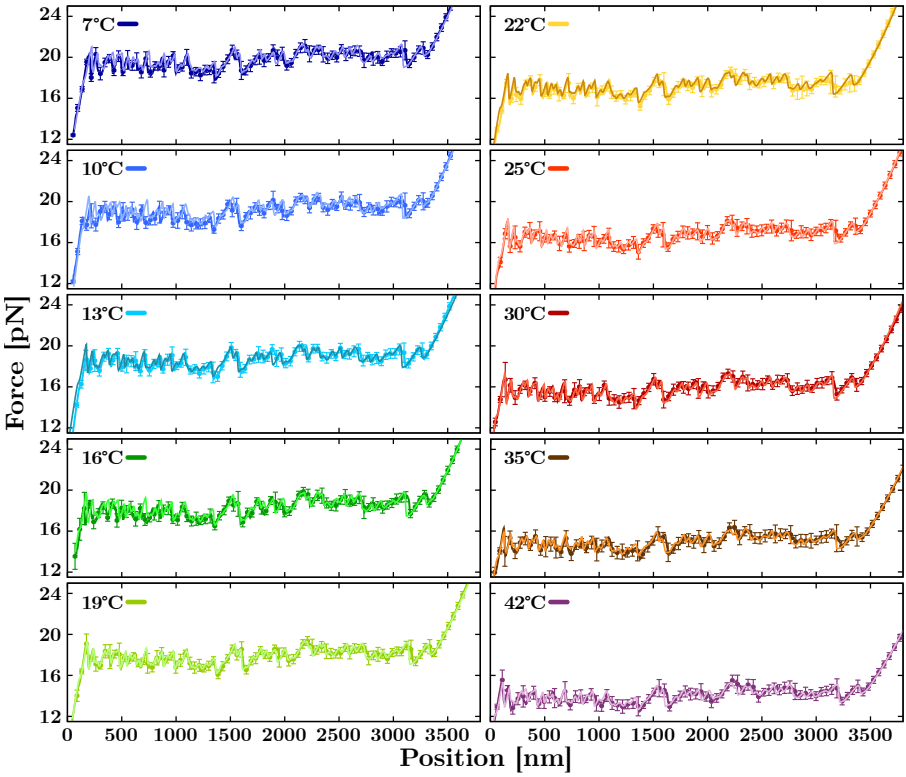

Supplementary Fig. 8: **T-dependence theoretical FDC predictions.** Experimental FDCs (dark-colored solid lines and points) and theoretical predictions (light-colored lines) obtained with the free energy parameters derived at each T. Error bars indicate the variability of the experimental FDCs. All data are presented as mean values +/− SE. Source data are provided as a Source Data file.

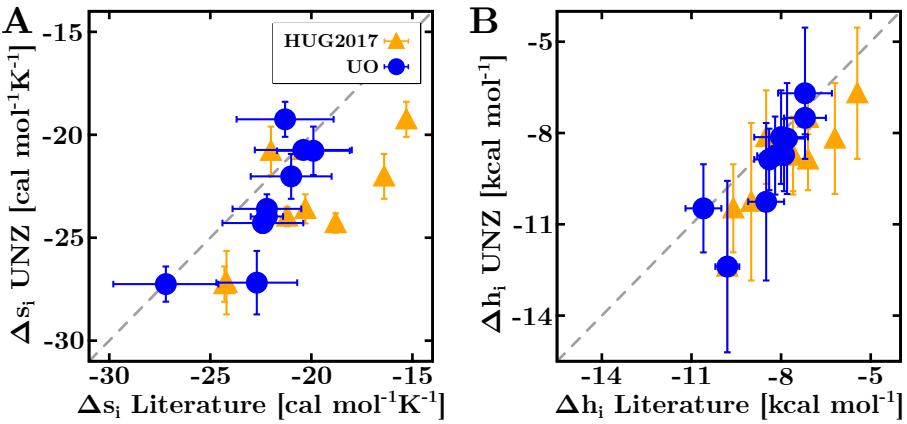

Supplementary Fig. 9: Comparison of the NNBP parameters with the literature. Correlation of NNBP unzipping (UNZ) parameters (y-axis) with the results (x-axis) by Huguet et al.[2] (orange) and Santalucia et al.[3] (blue) for the NNBP entropies, Δs_i (**A**), and enthalpies, Δh_i (**B**). Each point corresponds to a NNBP motif, a perfect correlation implying $x = y$ (dashed grey line). Notice that, since both the HUG2017 and UO datasets were obtained at different experimental conditions and $\Delta c_{p,i} = 0$, we compared these values to $\Delta s_{m,i}$ and $\Delta h_{m,i}$ extrapolated at T_m (main text, Fig. 4B at the bottom). All data are presented as mean values +/− SE. Source data are provided as a Source Data file.

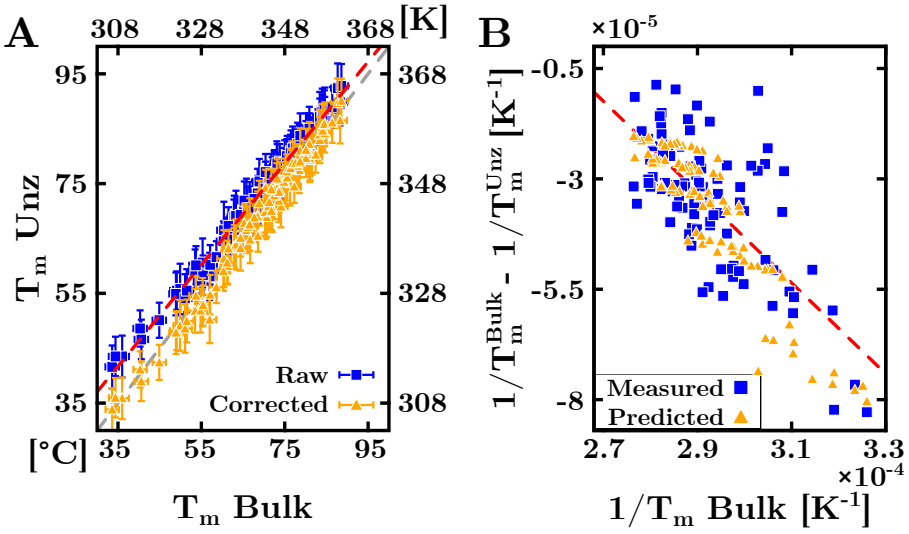

Supplementary Fig. 10: **Prediction of the DNA duplexes melting temperatures.** (**A**) Comparison of the melting temperatures for the set of 92 DNA oligos studied by Owczarzy et al. in Ref. [4] (horizontal axis) and the values predicted with the unzipping energy parameters (vertical axis). Perfect agreement between the two data sets would imply all points falling on the dashed grey line $x = y$. Predictions obtained with Eq.(10) of Sec. 6, Methods (blue squares) show a systematic discrepancy with respect to the experimental values (dashed red line). By accounting for the entropic correction (Eq.(11) of Sec. 6, Methods), predictions agree with the experimental measurements within errors (orange triangles). Results are reported in Supplementary Table 7. Data are presented as mean values +/− SE. (**B**) Derivation of the entropic correction, $\delta\Delta s$. To do this, we subtracted the inverse of the measured, T_m^{Bulk}, and predicted, T_m^{Unz}, melting temperatures (blue squares). This equals the difference between the inverse of Eq.(11) and Eq.(10) (see Eq.(12) in Sec. 6, Methods). A linear fit to data (dashed red line) yields $\delta\Delta s = 6(1)\,\mathrm{cal\,mol^{-1}K^{-1}} \sim 4R\log 2$, where $R = 1.987\,\mathrm{cal\,mol^{-1}K^{-1}}$ is the ideal gas constant. The orange triangles show the theoretical correction to T_m per DNA duplex predicted by assuming $\delta\Delta s \equiv 4R\log 2$. Source data are provided as a Source Data file.

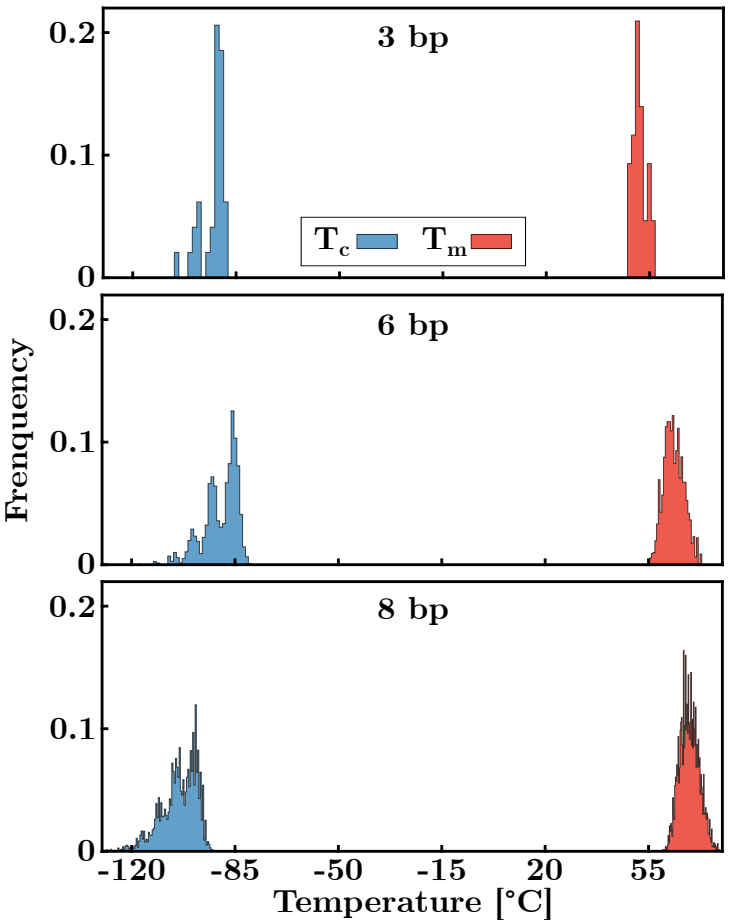

Supplementary Fig. 11: **Prediction of DNA cold denaturation temperatures.** Histograms of the melting (red) cold denaturation (blue) temperatures predicted using the ten NNBP thermodynamics parameters (Table 1, main text) for all possible DNA sequences of 3, 6, and 8 bp ending with a GAAA tetraloop. Source data are provided as a Source Data file.

Supplementary Tables

Supplementary Table 1: Oligo sequences

Oligo name	Sequence
Loop	5′ – Pho – AAT T GC CAG TTC GCG TTC GCC AGC ATC CG A CTA CGG ATG CTG GCG AAC GCG AAC TGG C – 3′
Bio-cosRshort3	5′ – Bio – GAC TTC ACT AAT ACG ACT CAC TAT AGG GA A ATA GAG ACA CAT ATA TAA TAG ATC TT – 3′
cosRlong	5′ – Pho – GGG CGG CGA CCT AAG ATC TAT TAT ATA TGT GTC TCT ATT AGT TAG TGG TGG AAA CAC AGT GCC AGC GC – Dig – 3′
Split3	5′ – TCC CTA TAG TGA GTC GTA TTA GTG AAG TC – 3′
Inverted-splint	3′ – Dig – AAA AA – 5′ – 5′ – GCG CTG GCA CTG TGT TTC CAC CAC TAA C (SpC3)– 3′

List of the oligo sequences used for the synthesis of the DNA hairpin.

Supplementary Table 2: **Hairpin sequence** ($5' \rightarrow 3'$)

ATAGAGACACATATATAATAGATCTTAGGTCGCCGCCCCGTAACCTGTCGGATCACC
GGAAAGGACCCGTAAAGTGATAATGATTATCATCTACATATCACAACGTGCGTGGAG
GCCATCAAACCACGTCAAATAATCAATTATGACGCAGGTATCGTATTAATTGATCTG
CATCAACTTAACGTAAAAACAACTTCAGACAATACAAATCAGCGACACTGAATACGG
GGCAACCTCATGTCAACGAAGAACAGAACCCGCAGAACAACAACCCGCAACATCCGC
TTTCCTAACCAAATGATTGAACAAATTAACATCGCTCTTGAGCAAAAAGGGTCCGGG
AATTTCTCAGCCTGGGTCATTGAAGCCTGCCGTCGGAGACTAACGTCAGAAAAGAGA
GCATATACATCAATTAAAAGTGATGAAGAATGAACATCCCGCGTTCTTCCCTCCGAA
CAGGACGATATTGTAAATTCACTTAATTACGAGGGCATTGCAGTAATTGAGTTGCAG
TTTTACCACTTTCCTGACAGTGACAGACTGCGTGTTGGCTCTGTCACAGACTAAATA
GTTTGAATGATTAGCAGTTATGGTGATCAGTCAACCACCAGGGAATAATCCTTCATA
TTATTATCGTGCTTCACCAACGCTGCCTCAATTGCTCTGAATGCTTCCAGAGACACCT
TATGTTCTATACATGCAATTACAACATCAGGGTAACTCATAGAAATGGTGCTATTAA
GCATATTTTTTACACGAATCAGATCCACGGAGGGATCATCAGCAGATTGTTCTTTAT
TCATTTTGTCGCTCCATGCGCTTGCTCTTCATCTAGCGGTTAAAATATTACTTCAAAT
CTTTCTGTATGAAGATTTGAGCACGTTGGCCTTACATACATCTGTCGGTTGTATTTC
CCTCCAGAATGCCAGCAGGACCGCACTTTGTTACGCAACCAATACTATTAAGTGAAA
ACATTCCTAATATTTGACATAAATCATCAACAAAACACAAGGAGGTCAGACCAGATT
GAAACGATAAAAACGATAATGCAAACTACGCGCCCTCGTATCACATGGAAGGTTTTA
CCAATGGCTCAGGTTGCCATTTTTAAAGAAATATTCGATCAAGTGCGAAAAGATTTA
GACTGTGAATTGTTTTATTCTGAACTAAAACGTCACAACGTCTCACATTATATTTACT
ATCTAGCCACAGATAATATTCACATCGTGTTAGAAAACGATAACACCGTGTTAATAA
AAGGACTTAAAAAGGTTGTAAATGTTAAATTCTCAAGAAACACGCATCTTATAGAAA
CGTCCTATGATAGGTTGAAATCAAGAGAAATCACATTTCAGCAATACAGGGAAAATC
TTGCTAAAGCAGGAGTTTTCCGATGGGTTACAAATATCCATGAACATAAAAGATATT
ACTATACCTTTGATAATTCATTACTATTTACTGAGAGCATTCAGAACACTACACAAAT
CTTTCCACGCTAAATCATAACGTCCGGTTTCTTCCGTGTCAGCACCGGGGCGTTGGC
ATAATGCAATACGTGTACGCGCTAAACCCTGTGTGCATCGTTTTAATTATTCCCGGA
CACTCCCGCAGAGAAGTTCCCCGTCAGGGCTGTGGACATAGTTAATCCGGGAATACA
ATGACGATTCATCGCACCTGACATACATTAATAAATATTAACAATATGAAATTTCAAC
TCATTGTTTAGGGTTTGTTTAATTTTCTACACATACGATTCTGCGAACTTCAAAAAGC
ATCGGGAATAACACCATGAAAAAAATGCTACTCGCTACTGCGCTGGCCCTGCTTATT
ACAGGATGTGCTCAACAGACGTTTACTGTTCAAAACAAACCGGCAGCAGTAGCACCA
AAGGAAACCATCACCCATCATTTCTTCGTTTCTGGAATTGGGCAGAAGAAAACTGTC
GATGCAGCCAAAATTTGTGGCGGCGCAGAAAATGTTGTTAAAACAGAAACCCAGCAA
ACATTCGTAAATGGATTGCTCGGTTTTATTACTTTAGGCATTTATACTCCGCTGGAA
GCGCGTGTGTATTGCTCACAATAATTGCATGAGTTGCCCATCGATATGGGCAACTCT
ATCTGCACTGCTCATTAATATACTTCTGGGTTCCTTCCAGTTGTTTTTGCATAGTGAT
CAGCCTCTCTCTGAGGGTGAAATAATCCCGTTCAGCGGTGTCTGCCAGTCGGGGGGA
GGCTGCATTATCCACGCCGGAGGCGGTGGTGGCTTCACGCACTGACTGACAGACTGC
TTTGATGTGCAACCGACGACGACCAGCGGCAACATCATCACGCAGAGCATCATTTTC
AGCTTTAGCATCAGCTAACTCCTTCGTGTATTTTGCATCGAGCGCAGCAACATCACG
CTGACGCATCTGCATGTCAGTAATTGCCGCGTTCGCCAGCTTCAGTTCTCTGGCATT
TTTGTCGCGCTGGGCTTTGTAGGTAATGGCGTTATCACGGTAATGATTAACAGCCCA
TGACAGGCAGACGATGATGCAGATAACCAGAGCGGAGATAATCGCGGTGACTCTGCT
CATACATCAATCTCTCTGACCGTTCCGCCCGCTTCTTTGAATTTTGCAATCAGGCTGT
CAGCCTTATGCTCGAACTGACCATAACCAGCGCCCGGCAGTGAAGCCCAGATATTGC
TGCAACGGTCGATTGCCTGACGGATATCACCACGATCAATCATAGGTAAAGCGCCAC
GCTCCTTAATCTGCTGCAATGCCACAGCGTCCTGACTTTTCGGAGAGAAGTCTTTCA
GGCCAAGCTGCTTGCGGTAGGCATCCCACCAACGGGAAAGAAGCTGGTAGCGTCCGG
CGCCTGTTGATTTGAGTTTTGGGTTTAGCGTGACAAGTTTGCGAGGGTGATCGGAGT
AATCAGTAAATAGCTCTCCGCCTACAATGACGTCATAACCATGATTTCTGGTTTTCTG
ACGTCCGTTATCAGTTCCCTCCGACCACGCCAGCATATCGAGGAACGCCTTACGTTG
ATTATTGATTTCTACCATCTTCTACTCCGGCTTTTTTAGCAGCGAAGCGTTTGATAAG
CGAACCAATCGAGTCAGTACCGATGTAGCCGATAAACACGCTCGTTATATAAGCGAG
ATTGCTACTTAGTCCGGCGAAGTCGAGAAGGTCACGAATGAACCAGGCGATAATGGC
GCACATCGTTGCGTCGATTACTGTTTTTGTAAACGCACCGCCATTATATCTGCCGCG
AAGGTACGCCATTGCAAACGCAAGGATTGCCCCGATGCCTTGTTCCTTTGCCGCGAG
AATGGCGGCCAACAGGTCATGTTTTTCTGGCATCTTCATGTCTTACCCCCAATAAGG
GGATTTGCTCTATTTAATTAGGAATAAGGTCGATTACTGATAGAACAAATCCAGGCT
ACTGTGTTTAGTAATCAGATTTGTTCGTGACCGATATGCACGGGCAAAACGGCAGGA
GGTTGTTAGCGCGACCTCCTGCCACCCGCTTTCACGAAGGTCATGTGTAAAAGGCCG
CAGCGTAACTATTACTAATGAATTGCCAGTTCGCGTTCGCCAGCATCCG

Sequence of the 3593bp Watson-Crick fully complementary DNA hairpin.

Supplementary Table 3: T-dependence of the DNA FDCs

T [°C]	**T [K]**	$\mathbf{f_m}$ **[pN]**	$\mathbf{l_p}$ **[nm]**	$\mathbf{d_b}$ **[nm]**	$\mathbf{\Delta s_{ss}}$ **[cal mol^{-1}K^{-1}]**
7	280	19.72 (3)	0.74 (7)	0.647 (3)	3.33 (2)
10	283	19.08 (4)	0.68 (2)	0.631 (9)	3.18 (2)
13	286	18.71 (4)	0.73 (3)	0.662 (1)	3.07 (2)
16	289	18.26 (7)	0.67 (2)	0.672 (1)	2.95 (2)
19	292	17.87 (4)	0.78 (2)	0.655 (1)	2.84 (2)
22	295	17.12 (2)	0.79 (3)	0.657 (1)	2.67 (2)
25	298	16.75 (3)	0.77 (2)	0.647 (1)	2.58 (2)
30	303	15.86 (2)	0.75 (2)	0.665 (1)	2.39 (2)
35	308	14.96 (3)	0.87 (2)	0.639 (1)	2.21 (1)
42	315	14.06 (4)	0.88 (4)	0.641 (1)	2.02 (1)

FDC average unzipping force, $f_{\rm m}$, persistence length, l_p, interphosphate distance, d_b, and ssDNA stretching entropy per base, Δs_{ss} in the studied temperature range (in Celsius and Kelvin degrees). All data are presented as mean values +/− SE (reported in brackets and referring to the last digit). The SE in temperature is ±1°C (K). Source data are provided as a Source Data file.

Supplementary Table 4: NNBP $\Delta s_{0,i}$ [cal mol^{-1}K^{-1}] at different temperatures.

Temperature ±1 [K]	**280**	**283**	**285**	**288**	**291**	**295**	**298**	**303**	**308**	**315**
AA/TT	-12.4 (6)	-12.6 (7)	-15.7 (5)	-13 (1)	-15.0 (3)	-16.0 (5)	-16.3 (4)	-16.9 (1)	-16.0 (4)	-18.3 (1)
AC/TG	-15.4 (7)	-15.6 (6)	-16.4 (6)	-16.4 (7)	-16.9 (4)	-17.5 31)	-17.7 (4)	-18.3 (2)	-18.6 (1)	-19.6 (1)
AG/TC	-12.0 (7)	-13.1 (6)	-11.8 (6)	-14.3 (2)	-13.3 (6)	-13.8 (6)	-14.5 (5)	-15.0 (5)	-16.2 (2)	-16.6 (3)
AT/TA	-15.1 (4)	-15.3 (3)	-16.1 (3)	-15.6 (6)	-16.4 (2)	-17.1 (3)	-16.7 (2)	-17.3 (1)	-17.3 (2)	-17.9 (1)
CA/GT	-13 (1)	-13.7 (9)	-13.7 (9)	-14.9 (5)	-15.1 (8)	-16.6 (4)	-16.0 (5)	-17.3 (4)	-19.3 (4)	-18.4 (3)
CC/GG	-12.4 (7)	-13.3 (6)	-12.2 (8)	-14.6 (1)	-13.5 (6)	-13.7 (4)	-14.8 (3)	-15.2 (5)	-16.0 (2)	-16.4 (2)
CG/GC	-22.2 (5)	-22.4 (4)	-21.4 (5)	-23.8 (1)	-22.8 (4)	-22.6 (3)	-23.7 (2)	-24.1 (4)	-24.2 (1)	-24.6 (2)
GA/CT	-12.4 (8)	-13.4 (6)	-12.4 (7)	-14.6 (5)	-14.0 (6)	-14.5 (6)	-14.7 (6)	-15.2 (6)	-16.6 (4)	-17.2 (2)
GC/CG	-20.8 (7)	-21.3 (6)	-19.7 (7)	-22.8 (4)	-21.5 (6)	-21.8 (3)	-22.7 (2)	-23.5 (5)	-24.4 (2)	-23.7 (3)
TA/AT	-16.1 (2)	-16.1 (2)	-17.1 (1)	-16.2 (6)	-16.9 (1)	-17.2 (3)	-17.5 (1)	-17.7 (1)	-16.7 (1)	-18.2 (1)

The 10 DNA entropies measured from unzipping a 3.6kbp hairpin in the temperature range $[280, 315]$ K (see text). The entropy of the last two motifs (GC/CG and TA/AT) has been computed by applying the circular symmetry relations. All data are presented as mean values +/− SE (reported in brackets and referring to the last digit). Source data are provided as a Source Data file.

Supplementary Table 5: NNBP $\Delta g_{0,i}$ [kcal mol^{-1}] at different temperatures.

Temperature ±1 [K]	**280**	**283**	**285**	**288**	**291**	**295**	**298**	**303**	**308**	**315**
AA/TT	-1.57 (5)	-1.49 (5)	-1.55 (5)	-1.47 (4)	-1.43 (4)	-1.43 (4)	-1.30 (4)	-1.27 (4)	-1.19 (4)	-1.15 (4)
AC/TG	-1.52 (5)	-1.38 (4)	-1.53 (5)	-1.35 (4)	-1.47 (4)	-1.34 (4)	-1.43 (4)	-1.36 (4)	-1.17 (4)	-1.21 (4)
AG/TC	-1.73 (5)	-1.66 (5)	-1.49 (5)	-1.60 (5)	-1.54 (5)	-1.42 (4)	-1.41 (4)	-1.25 (4)	-1.35 (4)	-1.25 (4)
AT/TA	-1.37 (4)	-1.43 (4)	-1.27 (4)	-1.32 (4)	-1.25 (4)	-1.28 (4)	-1.17 (4)	-1.00 (3)	-1.19 (4)	-1.00 (3)
CA/GT	-1.86 (6)	-1.92 (6)	-1.82 (6)	-1.88 (6)	-1.82 (6)	-1.91 (6)	-1.65 (5)	-1.68 (5)	-1.70 (5)	-1.52 (5)
CC/GG	-2.03 (6)	-1.86 (6)	-2.04 (6)	-1.91 (6)	-2.00 (6)	-1.88 (6)	-1.91 (6)	-1.86 (6)	-1.56 (5)	-1.70 (5)
CG/GC	-2.51 (8)	-2.52 (8)	-2.39 (7)	-2.46 (7)	-2.35 (7)	-2.24 (7)	-2.43 (7)	-2.30 (7)	-2.03 (6)	-1.93 (6)
GA/CT	-1.52 (5)	-1.59 (5)	-1.55 (5)	-1.48 (4)	-1.49 (5)	-1.42 (4)	-1.52 (5)	-1.46 (4)	-1.26 (4)	-1.20 (4)
GC/CG	-2.79 (8)	-2.83 (9)	-2.51 (8)	-2.78 (8)	-2.55 (8)	-2.53 (8)	-2.49 (8)	-2.36 (7)	-2.34 (7)	-2.11 (6)
TA/AT	-1.31 (4)	-1.19 (4)	-1.10 (3)	-1.11 (3)	-1.10 (3)	-1.00 (3)	-1.00 (3)	-0.74 (2)	-0.97 (3)	-0.88 (3)

The 10 DNA free-energies measured from unzipping a 3.6kbp hairpin in the temperature range $[280, 315]$ K (see text). The entropy of the last two motifs (GC/CG and TA/AT) has been computed by the applying circular symmetry relations. All data are presented as mean values +/− SE (reported in brackets and referring to the last digit). Source data are provided as a Source Data file.

Supplementary Table 6: NNBP $\Delta h_{0,i}$ [kcal mol^{-1}] at different temperatures.

Temperature ±1 [K]	**280**	**283**	**285**	**288**	**291**	**295**	**298**	**303**	**308**	**315**
AA/TT	-5.0 (3)	-5.0 (3)	-6.0 (3)	-5.2 (6)	-5.8 (2)	-6.2 (3)	-6.2 (3)	-6.4 (1)	-6.1 (2)	-6.9 (1)
AC/TG	-5.8 (3)	-5.8 (3)	-6.2 (3)	-6.1 (3)	-6.4 (3)	-6.5 (2)	-6.7 (3)	-6.9 (2)	-6.9 (1)	-7.4 (2)
AG/TC	-5.1 (4)	-5.4 (3)	-4.9 (3)	-5.7 (2)	-5.4 (3)	-5.5 (3)	-5.7 (3)	-5.8 (3)	-6.3 (2)	-6.5 (2)
AT/TA	-5.6 (2)	-5.8 (2)	-5.8 (2)	-5.8 (3)	-6.0 (2)	-6.3 (2)	-6.1 (2)	-6.3 (1)	-6.5 (2)	-6.6 (1)
CA/GT	-5.4 (5)	-5.8 (4)	-5.7 (4)	-6.2 (3)	-6.2 (4)	-6.8 (3)	-6.4 (3)	-6.9 (3)	-7.7 (3)	-7.3 (2)
CC/GG	-5.5 (4)	-5.6 (4)	-5.5 (4)	-6.1 (2)	-5.9 (4)	-5.9 (3)	-6.3 (3)	-6.4 (3)	-6.5 (2)	-6.9 (2)
CG/GC	-8.7 (4)	-8.6 (4)	-8.5 (4)	-9.3 (2)	-9.0 (3)	-8.9 (3)	-9.5 (3)	-9.6 (4)	-9.5 (2)	-9.7 (3)
GA/CT	-5.0 (4)	-5.4 (3)	-5.1 (3)	-5.7 (3)	-5.6 (3)	-5.7 (3)	-5.9 (3)	-6.1 (3)	-6.4 (2)	-6.6 (2)
GC/CG	-8.6 (5)	-8.8 (4)	-8.1 (4)	-9.4 (2)	-8.8 (3)	-9.0 (3)	-9.3 (3)	-9.5 (4)	-9.9 (3)	-9.6 (3)
TA/AT	-5.8 (2)	-5.7 (2)	-6.0 (2)	-5.8 (3)	-6.0 (1)	-6.1 (2)	-6.2 (1)	-6.1 (1)	-6.1 (1)	-6.6 (1)

The 10 DNA enthalpies measured from unzipping a 3.6kbp hairpin in the temperature range $[280, 315]$ K (see text). The entropy of the last two motifs (GC/CG and TA/AT) has been computed by the applying circular symmetry relations. All data are presented as mean values +/− SE (reported in brackets and referring to the last digit). Source data are provided as a Source Data file.

Supplementary Table 7: DNA Oligos Melting Temperatures [°C]

Sequence ($5' \rightarrow 3'$)	$\mathbf{T^{Exp}}$	$\mathbf{T^{Unz}_{Bi}}$	$\mathbf{T^{Unz}_{Uni}}$	$\mathbf{T^{UO}}$	$\mathbf{T^{Hug}}$
ATCAATCATA	33.6	39.9	32.4	33.8	32.3
TTGTAGTCAT	36.0	41.9	34.6	35.9	36.2
GAAATGAAAG	34.4	42.6	35.7	36.0	33.8
CCAACTTCTT	40.6	45.2	38.1	39.0	38.9
ATCGTCTGGA	44.9	48.3	40.9	42.4	45.3
AGCGTAAGTC	40.3	47.1	40.1	41.1	43.4
CGATCTGCGA	49.1	53.8	46.9	48.2	50.2
TGGCGAGCAC	55.3	58.8	52.0	53.4	54.7
GATGCGCTCG	53.5	57.3	50.7	51.8	52.9
GGGACCGCCT	57.0	56.2	48.8	50.2	55.3
CGTACACATGC	49.9	54.3	48.1	49.1	50.6
CCATTGCTACC	48.9	53.4	46.9	47.8	48.2
TACTAACATTAACTA	51.1	52.8	47.5	48.6	50.1
ATACTTACTGATTAG	51.5	54.2	48.9	50.0	50.4
GTACACTGTCTTATA	54.8	56.0	50.8	51.9	54.2
GTATGAGAGACTTTA	55.4	57.0	51.8	52.8	54.2
TTCTACCTATGTGAT	53.7	58.8	53.5	54.6	55.7
AGTAGTAATCACACC	57.1	58.8	53.6	54.8	57.2
ATCGTCTCGGTATAA	58.6	60.3	55.0	56.1	59.9
ACGACAGGTTTACCA	61.3	63.9	58.7	60.0	63.6
CTTTCATGTCCGCAT	62.8	66.9	61.9	63.3	62.6
TGGATGTGTGAACAC	60.4	65.0	60.1	61.3	62.1
ACCCCGCAATACATG	62.9	67.3	62.2	63.6	64.5
GCAGTGGATGTGAGA	63.3	67.5	62.5	63.9	64.2
GGTCCTTACTTGGTG	60.3	62.9	57.8	59.1	61.7
CGCCTCATGCTCATC	65.8	69.9	65.1	66.5	65.9
AAATAGCCGGGCCGC	70.4	72.9	67.8	69.3	70.9
CCAGCCAGTCTCTCC	66.7	68.4	63.4	64.8	66.7
GACGACAAGACCGCG	68.6	68.9	64.1	65.5	70.3
CAGCCTCGTCGCAGC	72.0	73.6	68.9	70.5	72.7
CTCGCGGTCGAAGCG	70.7	72.2	67.4	68.9	73.6
GCGTCGGTCCGGGCT	74.1	74.4	69.4	70.8	76.1
TATGTATATTTTGTAATCAG	61.2	63.7	59.7	60.6	59.5
TTCAAGTTAAACATTCTATC	61.5	66.1	62.1	63.2	62.6
TGATTCTACCTATGTGATTT	64.4	68.2	64.1	65.1	64.8
GAGATTGTTTCCCTTTCAAA	65.3	70.7	66.8	67.8	67.1
ATGCAATGCTACATATTCGC	68.9	74.1	70.3	71.4	69.6
CCACTATACCATCTATGTAC	64.4	66.2	62.2	63.2	65.2
CCATCATTGTGTCTACCTCA	68.5	72.0	68.1	69.2	69.7
CGGGACCAACTAAAGGAAAT	68.5	71.8	67.8	69.0	70.5
TAGTGGCGATTAGATTCTGC	71.2	73.0	69.1	70.2	70.9
AGCTGCAGTGGATGTGAGAA	73.1	77.0	73.1	74.1	74.0
TACTTCCAGTGCTCAGCGTA	73.6	74.8	70.9	71.9	74.6
CAGTGAGACAGCAATGGTCG	72.5	75.3	71.5	72.8	73.9
CGAGCTTATCCCTATCCCTC	70.3	72.5	68.4	69.8	71.9
CGTACTAGCGTTGGTCATGG	71.1	73.4	69.6	70.8	74.0
AAGGCGAGTCAGGCTCAGTG	76.3	77.7	73.9	75.1	77.0
ACCGACGACGCTGATCCGAT	77.3	77.4	73.5	74.5	78.6
AGCAGTCCGCCACACCCTGA	78.5	80.3	76.4	77.5	79.7
CAGCCTCGTTCGCACAGCCC	78.1	80.5	76.8	78.3	80.4
GTGGTGGGCCGTGCGCTCTG	81.0	81.8	78.1	79.6	82.0
GTCCACGCCCGGTGCGACGG	81.1	81.6	77.8	79.3	84.2
GATATAGCAAAATTCTAAGTTAATA	66.1	69.5	66.2	67.1	65.9
ATAACTTTACGTGTGTGACCTATTA	71.8	72.5	69.2	70.0	72.4
GTTCTATACTCTTGAAGTTGATTAC	67.7	71.0	67.8	68.8	69.9
CCCTGCACTTTAACTGAATTGTTTA	72.5	76.0	72.8	73.8	73.5
TAACCATACTGAATACCTTTTGACG	71.3	73.9	70.7	71.6	73.0
TCCACACGGTAGTAAAATTAGGCTT	73.8	76.2	72.9	73.8	75.8
TTCCAAAAGGAGTTATGAGTTGCGA	73.8	78.1	74.9	75.7	76.2
AATATCTCTCATGCGCCAAGCTACA	76.5	80.0	76.8	77.6	77.3
TAGTATATCGCAGCATCATACAGGC	75.0	77.7	74.5	75.5	75.8
TGGATTCTACTCAACCTTAGTCTGG	73.6	75.7	72.4	73.5	75.2
CGGAATCCATGTTACTTCGGCTATC	74.8	77.3	74.1	75.3	76.6

Supplementary Table 7: DNA Oligos Melting Temperatures [°C]

Sequence ($5' \to 3'$)	$\mathbf{T^{Exp}}$	$\mathbf{T^{Unz}_{Bi}}$	$\mathbf{T^{Unz}_{Uni}}$	$\mathbf{T^{UO}}$	$\mathbf{T^{Hug}}$
CTGGTCTGGATCTGAGAACTTCAGG	75.6	78.2	75.0	76.1	77.3
ACAGCGAATGGACCTACGTGGCCTT	81.0	82.0	78.8	79.6	82.1
AGCAAGTCGAGCAGGGCCTACGTTT	81.5	82.6	79.4	80.2	82.8
GCGAGCGACAGGTTACTTGGCTGAT	80.1	81.8	78.7	79.7	81.7
AAAGGTGTCGCGGAGAGTCGTGCTG	82.4	82.3	79.2	80.3	83.6
ATGGGTGGGAGCCTCGGTAGCAGCC	83.4	85.0	81.8	82.9	84.6
CAGTGGGCTCCTGGGCGTGCTGGTC	83.4	85.7	82.6	83.9	85.7
GCCAACTCCGTCGCCGTTCGTGCGC	84.6	85.8	82.8	84.2	88.0
ACGGGTCCCCGCACCGCACCGCCAG	88.3	88.5	85.3	86.5	90.1
TTATGTATTAAGTTATATAGTAGTAGTAGT	66.6	69.8	66.9	67.5	69.7
ATTGATATCCTTTTCTATTCATCTTTCATT	70.4	76.4	73.6	74.2	71.8
AAAGTACATCAACATAGAGAATTGCATTTC	73.2	77.8	75.1	75.9	74.6
CTTAAGATATGAGAACTTCAACTAATGTGT	71.8	75.9	73.2	74.0	74.2
CTCAACTTGCGGTAAATAAATCGCTTAATC	75.5	78.9	76.2	77.2	77.3
TATTGAGAACAAGTGTCCGATTAGCAGAAA	76.4	79.8	77.1	77.8	78.4
GTCATACGACTGAGTGCAACATTGTTCAAA	76.9	80.4	77.8	78.7	79.3
AACCTGCAACATGGAGTTTTTGTCTCATGC	78.7	82.8	80.2	81.0	80.1
CCGTGCGGTGTGTACGTTTTATTCATCATA	77.6	80.5	77.8	78.7	80.5
GTTCACGTCCGAAAGCTCGAAAAAGGATAC	78.7	80.6	78.0	79.0	81.5
AGTCTGGTCTGGATCTGAGAACTTCAGGCT	80.6	83.0	80.2	80.9	82.5
TCGGAGAAATCACTGAGCTGCCTGAGAAGA	80.9	84.2	81.5	82.2	83.3
CTTCAACGGATCAGGTAGGACTGTGGTGGG	80.1	82.7	80.0	81.2	83.4
ACGCCCACAGGATTAGGCTGGCCCACATTG	84.0	87.1	84.4	85.3	85.5
GTTATTCCGCAGTCCGATGGCAGCAGGCTC	84.1	86.2	83.6	84.7	85.6
TCAGTAGGCGTGACGCAGAGCTGGCGATGG	84.6	87.4	84.8	85.8	88.2
CGCGCCACGTGTGATCTACAGCCGTTCGGC	84.5	87.3	84.7	85.8	89.3
GACCTGACGTGGACCGCTCCTGGGCGTGGT	86.4	87.8	85.1	86.1	89.9
GCCCCTCCACTGGCCGACGGCAGCAGGCTC	87.7	91.0	88.4	89.6	91.5
CGCCGCTGCCGACTGGAGGAGCGCGGGACG	88.6	91.4	88.8	90.1	93.9

Melting temperatures of the 92 DNA duplexes studied by Owczarzy et al. in Ref.[4] at a concentration $c = 2\mu$M and 1020mM NaCl. The experimental values ($T^{\rm Exp}$) are compared with predictions obtained with the unzipping parameters by using Eq.(10) ($T^{\rm Unz}_{\rm Bi}$) and Eq.(11) ($T^{\rm Unz}_{\rm Uni}$) for bimolecular and unimolecular reactions, respectively (see main text and Sec. 6, Methods). Finally, $T^{\rm UO}$ and $T^{\rm Hug}$ are obtained with the unified oligonucleotide parameters (UO) in Ref.[3] and the Huguet et al. (2017) parameters in Ref.[2]. Results are reported with errors: $T^{\rm Exp} \pm 1.6$°C, $T^{\rm Unz} \pm 1.5$°C, $T^{\rm UO} \pm 1.5$°C, and $T^{\rm Hug} \pm 1.5$°C. Temperatures are given in Celsius degrees. Source data are provided as a Source Data file.

Supplementary Methods

1 Synthesis of the 3.6kbp DNA Hairpin

To carry out the unzipping experiments with the temperature-jump optical trap, we designed and synthesized a 3593bp DNA hairpin ending with a GAAA tetraloop. This hairpin is flanked by two 29bp dsDNA handles tagged with biotin and digoxigenin at the other end to increase the tether lifetimes. The synthesis steps are described in red below.

Restriction Digest of λ-DNA

We start by digesting the N6-methyladenine-free λ-DNA using the restriction enzyme EcoRI from New England Biolabs. The fragment spanning positions from 44972 to 48502 on the cosR end of the λ-DNA has been used to assemble the hairpin stem. The digestion reaction was prepared as follows:

Components. 64μl MilliQ water, 10μl 10X NEB reaction buffer, 1μl 100X BSA, 20μl λ-DNA (0.5μg/μl), and 5μl EcoRI enzyme (20U/μl).

Procedure. The reaction was incubated for 3 hours at 37°C to ensure complete digestion. Next, EcoRI was thermally inactivated at 65°C for 20min.

The EcoRI restriction enzyme has been used to cut the λ-DNA into six fragments of lengths 21226bp, 7421bp, 5804bp, 5643bp, 4878bp, and 3530bp. Then, the digested DNA was purified (0.8% agarose gel, 1XTBE) using Sybr Safe staining (5μl) and blue illumination to minimize DNA damage and nicking. Finally, the 3530bp fragment was extracted using the Qiaquick gel extraction kit (Qiagen). The purified DNA was eluted in 50μl of 2mM Tris-Cl.

Phosphorylation of Digested λ-DNA

The digested λ-DNA fragment was phosphorylated using T4 polynucleotide kinase to prepare it for subsequent ligation. The phosphorylation reaction included:

Components. 19μl MilliQ water, 10μl 10X PNK buffer, 10μl, 10mM ATP, 50μl of digested λ-DNA (≈180ng/μl) and 1μl of T4 polynucleotide kinase.

Procedure. The reaction was incubated for 30 minutes at 37°C. Next, polynucleotide kinase was thermally inactivated at 65°C for 20min.

Synthesis of dsDNA Handles and End-Loop

To create the hairpin structure, the phosphorylated λ-DNA fragment was annealed to oligonucleotides that form the hairpin loop and the dsDNA handles. The end-loop was synthesized by annealing the DNA fragment to an oligonucleotide (Oligonucleotide loop in Supplementary Table 1), which

self-assembled into a hairpin with a tetraloop at one end and an overhang complementary to the EcoRI restriction site. The dsDNA handles were formed using two partially complementary oligonucleotides (cosRlong and Bio-cosRshort3 in Supplementary Table 1) that hybridize forming a protruding end complementary to the cosR end. The Bio-cosRshort3 oligonucleotide was purchased 5′-biotinylated. The molecular construction was doubly biotinylated in one handle and doubly Digoxigenin-tailed in the other handle.

Double Biotinylated Handle. Bio-cosRshort3, and the complementary oligonucleotide (Split3 in the Supplementary Table 1) were tailed at the 3′ end with multiple biotins using terminal transferase and biotin-labeled dUTPs (Roche).

Double Digoxigenin-Tailed Handle. To create the digoxigenin dsDNA handle, we used cosR-long oligocleotide and a modified oligonucleotide (inverted-splint Supplementary Table 1) complementary to the unpaired region of cosRlong. This oligonucleotide was modified with a polarity inversion at its 5′ end and a blocked 3′ end which allowed the oligonucleotide to be tailed with multiple digoxigenins at its 5′ end using digoxigenin-labeled dUTPs (Roche).

Oligonucleotide Tailing

The tailing reactions for both the biotin and digoxigenin-modified oligonucleotides were prepared using terminal transferase. The reaction mixture included:

Components. 8μl MilliQ water, 4μl 5X $CoCl_2$ solution, 4μl 5X reaction buffer, 1μl 10mM dATP, 1μl of either 1mM BIO-dUTP or DIG-dUTP (Roche), and 1μl 100μM oligonucleotide.

Procedure. The reaction was incubated for 15 minutes at 37°C, followed by the addition of 1μl of 0.5M EDTA to stop the reaction. The tailed oligonucleotides were purified using the QIAquick Nucleotide Removal Kit (Qiagen) and eluted in 50μl of 10mM Tris-Cl.

Annealing of the DNA Hairpin

Once the oligonucleotides for the handles and the end-loop were prepared, they were annealed to the phosphorylated λ-DNA fragment in a reaction containing:

Components. 29μl digested λ-DNA (330ng/μl), 5μl of each oligonucleotide (at varying concentrations for the loop and handles), 1.5μl 1M Tris pH 7.5, and 1.2μl 5M NaCl.

Procedure. The reaction was incubated at 70°C for 10 minutes, then at

55°C for 10 minutes, and gradually cooled down to room temperature in a thermal bath.

Ligation of the DNA Hairpin

Finally, the annealed hairpin construct was ligated overnight using T4 DNA ligase in the following ligation reaction:

Components. 55μl annealed product, 8μl 10X T4 DNA ligase buffer, 5μl 10mM ATP, and 3μl T4 DNA ligase (400U/μl).

Procedure. The reaction was incubated overnight at 16°C. After ligation, the reaction was thermally inactivated by incubating at 65°C for 10 minutes, and the final product was stored at −20°C.

This procedure resulted in the synthesis of a 3.6kbp DNA hairpin structure, ready for use in force-spectroscopy. The hairpin sequence is reported in Supplementary Table 2.

2 The Effective Stiffness Method

The elastic properties of ssDNA are strongly temperature dependent (see Fig. 1B, main text). Accurately measuring the elastic parameters requires modeling all contributions to the trap-pipette distance, λ, which includes the optical trap displacement ($x_{\rm b}$), the dsDNA handles ($x_{\rm h}$), the ssDNA ($x_{\rm ss}$), and the molecular diameter (d_0). The setup contributions ($x_{\rm b}$ and $x_{\rm h}$) have been evaluated according to the effective stiffness method[5], by which are treated as serially connected springs so that $k_{\rm eff}^{-1} = k_{\rm b}^{-1} + k_{\rm h}^{-1}$. Both terms can be considered force-independent in the explored range of forces ($\sim 0 - 25$pN). In fact, the trapped bead is subject to a harmonic potential $\propto k_b x^2$ so that it has a linear response with force. In general, deviations from the linearity of the optical trap are minor, with k_b increasing by $\sim 5\%$ from 0 to 20pN[6], within statistical errors. Moreover, as the force varies in a relatively narrow range ($f_{\rm max} - f_{\rm min} \lesssim 10$pN), the trap stiffness can be considered nearly force-independent so $k_{\rm eff}$ is constant along the folded branch of the FDC. The contribution from the dsDNA short handles (29bp each), $k_{\rm h}$, can be neglected as they become fully stretched at low forces (2-3pN), behaving as rigid rods with $k_h \gg k_{\rm b}$. Thus, for all practical purposes $k_{\rm eff}^{-1} \approx k_{\rm b}^{-1}$ or $k_{\rm eff} \approx k_{\rm b}$.

We computed $k_{\rm eff}$ by fitting the slope preceding the first force rip in the FDC to the linear equation $f = k_{\rm eff} x$ (orange dashed-line in Supplementary Fig. 3). For each temperature, we have measured $k_{\rm eff}$ by fitting the slope preceding the first FDC rip to a straight line. To better capture the variability of this parameter, we extracted it independently for each unzipping/rezipping trajectory and finally averaged the results over all molecules at a given T. In Supplementary Fig. 4A, B, we show the stiffness variability among trajectories

and molecules at 25°C, respectively. Results are compatible with the standard errors, proving that these measurements are sample-independent. Finally, in Supplementary Fig. 4C, we show k_{eff} averaged over all molecules at each studied temperature. It is apparent that the stiffness does not exhibit any temperature dependence.

3 Stochastic Gradient Descent in a Nutshell

The basic principle behind stochastic approximation can be backtracked to the Robbins–Monro algorithm of the 1950*s*[7]. Since then, stochastic gradient descent (SGD) methods have become one of the most widely used optimization methods[8–12]. SGD is an iterative method for optimizing an objective function, $J(w)$, with suitable smoothness properties (e.g., differentiable or subdifferentiable). The set of parameters, w^*, minimizing $J(w)$, is iteratively approximated according to an update algorithm proportional to the antigradient of the objective function, $-\nabla_w J(w)$. Starting from an initial guess of w, at each step of the algorithm, the parameters are updated according to

$$\begin{cases} w_{t+1} &= w_t + v_{t+1} \\ v_{t+1} &= \beta v_t - \eta \nabla_{w_t} J(w)\,, \end{cases} \tag{1}$$

where v_t is the velocity of the optimization and $\eta \geq 0$ is the step size (called learing rate). The parameter β (the so-called momentum coefficient) accounts for a fraction of the previous step in the current update. The critical difference between SGD and standard gradient descent algorithms is that information (total entropy and coefficients) from only one FEC segment (Δx_k) at a time is used to calculate the step, and the segment is picked randomly at each step.

The SGD convergence rate can be improved by considering Nesterov's Accelerated Gradient (NAG), introduced in 1983[13,14]. According to NAG, the update equations are

$$\begin{cases} w_{t+1} &= w_t + v_{t+1} \\ v_{t+1} &= \beta v_t - \eta \nabla_{w_t + \beta v_t} J(w)\,. \end{cases} \tag{2}$$

While the classic momentum (CM) algorithm updates the velocity vector by computing the gradient at w_t, the NAG algorithm computes the gradient at $w_t + \beta v_t$. To make an analogy, while CM faithfully trusts the gradient at the current iteration, NAG puts less faith in it and looks ahead in the direction suggested by the velocity vector; it then moves in the direction of the gradient at the look-ahead point. If $\nabla_{w_t+\beta v_t} J(w) \approx \nabla_{w_t} J(w)$, then the two updates are similar. The advantage of using NAG is that it converges at a rate of $\mathcal{O}(1/t^2)$, while CM converges at a rate of $\mathcal{O}(1/t)$.

To derive the DNA NNBP entropies from unzipping experiments, we used an SGD minimization implementing NAG update equations. Let us rewrite

Eq.(2) (main text) as $\mathbf{\Delta S_0} = C\mathbf{\Delta s}$, where $\mathbf{\Delta S_0}$ is the vector of entropies measured with the Clausius-Clapeyron equation for each of the K FEC segments, $\mathbf{\Delta s}$ is the vector of the $I = 8$ NNBP entropy parameters, and C is the $K \times I$ matrix of the coefficients, $c_{k,i}$.

Thus, for a given loss function (ex., least squares), the algorithm has to minimize

$$J(w) = \sum_{k=1}^{K} (\hat{w}_k - w_k)^2 = \sum_{k=1}^{K} (\Delta S_{0,k} - C_k \mathbf{\Delta s})^2 \,. \tag{3}$$

By using this method, we measured the DNA entropies at the single base-pair level for each experimental temperature in the range $[280, 315]$ K (see results in Fig. 3C, main text and Supplementary Table 4).

4 Prediction of the DNA Unzipping Curve

In unzipping experiments, the total trap–pipette distance, λ, can be written as

$$\lambda(f) = x_{\rm b}(f) + x_{\rm h}(f) + x_{\rm ss}(f, n) + x_{\rm d}(f) \,, \tag{4}$$

where $x_{\rm b}(f)$ is the displacement of the bead from the center of the optical trap, $x_{\rm h}(f)$ and $x_{\rm ss}(f, n)$ account for the extension of the two double-stranded handles and the ssDNA extension, respectively (described with the WLC model, Eq.(5), Methods), and $x_{\rm d}(f)$ is the projection of the folded hairpin of diameter d (typically $d = 2$nm for DNA and RNA hairpins[15]) along the pulling axis[6]. It is modeled with the freely-jointed chain in Eq.(6), Methods. For a given λ, the total system free energy is given by

$$\begin{aligned} \Delta G_{\rm tot}(\lambda, n) = & \Delta G_0(n) + \Delta G_{\rm b}(x_{\rm b}) + \Delta G_{\rm h}(x_{\rm h}) + \\ & + \Delta G_{\rm ss}(x_{\rm ss}, n) + \Delta G_{\rm d}(x_{\rm d}) \,, \end{aligned} \tag{5}$$

where $\Delta G_0(n) = \sum_i^n \Delta g_{0,i}$, is the hairpin free-energy of hybridization according to the NN model and the other terms are the energy contributions of the corresponding elastic terms in Eq.(4)

4.1 Computation of the Equilibrium FDC

Let us consider the case where thermal fluctuations are neglected in the FDC computation. Thus, at a given value of λ, the system is always in the state of minimum energy, $\Delta G_{\rm eq}(\lambda) = \Delta G_{\rm tot}(\lambda, n^*)$. To compute the equilibrium free energy of the system, let us first introduce the system partition function, Z. At each λ, this is defined as the sum over all the possible states, i.e., all the possible sequences of n open base pairs, which is

$$Z(\lambda) = \sum_{n=0}^{N} \exp\left(-\frac{\Delta G_{\rm tot}(\lambda, n)}{k_{\rm B} T} \right) \,, \tag{6}$$

where N is the total number of base pairs of the sequence. Finally, by recalling that $\Delta G = -k_{\mathrm{B}}T \ln Z$, the equilibrium force is given by:

$$f_{\mathrm{eq}}(\lambda) \equiv \frac{\partial \Delta G(x_{\mathrm{eq}})}{\partial \lambda} = -k_{\mathrm{B}}T \frac{\partial \ln Z(\lambda)}{\partial \lambda}. \tag{7}$$

Computing Eq.(6) requires solving the transcendental Eq.(4) with respect to f (that can be performed numerically) and then computing Eq.(5) for all $n \in [0, N-1]$. For each λ, the value n^* minimizing the equilibrium free-energy $\Delta G_{\mathrm{eq}} = \Delta G_{\mathrm{tot}}(\lambda, n^*(\lambda))$ gives the most probable number of open base-pairs. Eventually, the computation of the equilibrium force in Eq.(7) gives the FDC theoretical prediction at a given T (Supplementary Fig. 8).

4.2 Equilibrium Free Energy

The total free energy in Eq.(5) is the sum of two main contributions: the hybridization energy $\Delta G_0(n)$, which linearly depends on the number of hybridized NNBPs n, and the stretching energy $\Delta G_{\mathrm{el}}(\lambda, n) = \Delta G_{\mathrm{b}}(x_{\mathrm{b}}) + \Delta G_{\mathrm{h}}(x_{\mathrm{h}}) + \Delta G_{\mathrm{ss}}(x_{\mathrm{ss}}, n) + \Delta G_{\mathrm{d}}(x_{\mathrm{d}})$ depending on both n and λ. For a given λ, the equilibrium configuration of the system is that with minimum $\Delta G_{\mathrm{el}}(\lambda, n^*)$ and maximum $\Delta G_0(n^*)$ among all possible values of n. Notice that for a hairpin of N bp, n ranges from 0 (native state) to $N-1$ NNBPs (totally unfolded), which gives $N-1$ possible system configurations for each value of λ.

Let us suppose that the system starts at equilibrium, with n_1 open bp. Upon increasing λ, the elastic term in Eq.(5) also increases. The number of open bp, n_1, remains constant until a value of $n = n_2 > n_1$ is found so that $\Delta G_{\mathrm{tot}}(\lambda, n_1) \equiv \Delta G_{\mathrm{tot}}(\lambda, n_2)$ (Supplementary Fig. 7A, top): even though the total energy of these two states is the same, the energetic internal balance is different (Supplementary Fig. 7A, bottom). The system minimizes the elastic free energy and switches to state n_2 by releasing $\Delta n = n_2 - n_1$ bp. Notice that, despite opening Δn bp increases the system's energy, the released ssDNA causes the elastic contribution to decrease. In general, $\Delta G_{\mathrm{el}} \gg \Delta G_0$ so the global balance of the state n_2 is lower than the one of n_1. Therefore, the equilibrium free energy of hybridization, $\Delta G_0(n*)$, is a step function increasing with λ (Supplementary Fig. 7B) with each discontinuity corresponding to a rip along the equilibrium FDC.

5 Error derivation of the NNBP parameters

Statistical error estimation is crucial to our analysis, where the measured thermodynamic parameters depend on several variables, each with its uncertainty. The stochastic nature of the gradient descent algorithm allowed us to derive the NNBP entropies and compute the standard deviation of the parameters with the bootstrap method. Bootstrapping is a statistical method that involves repeatedly sampling from a dataset to estimate the distribution of a set of parameters. It permits us to estimate the variability and confidence intervals of the parameters without making strong assumptions about the underlying

distributions. For example, the standard deviations reported for the entropy values in the figures and tables have been derived by performing 10^3 bootstrap resampling for the data at each temperature. An analogous argument can be made for the Monte Carlo minimization algorithm to determine the NNBP free energies. However, the main uncertainty in the NNBP parameters derivation using force spectroscopy comes from the measurement of the ssDNA elastic response. It has been shown[16] that the total error in determining the energy parameters is dominated by the uncertainty of the ssDNA elastic parameters: a $5-10\%$ error in the estimation of the persistence length of ssDNA translates into a similar error in the NNBP energies. This yields an accuracy of ≈ 0.1kcal/mol in estimating the NNBP free energies.

To determine the statistical errors, we have propagated the values of the elastic parameters at the limits of their confidence interval to determine the corresponding free energies, enthalpies, and entropies at all temperatures. Minimum and maximum values for $\Delta g_i(T)$, $\Delta s_i(T)$, and $\Delta h_i(T)$ set the confidence intervals on each quantity with the corresponding mean (see Supplementary Tables 4, 5, and 6). Once $\Delta s_i(T)$ and $\Delta h_i(T)$ were determined with their statistical errors, the standard errors of the thermodynamic parameters in Table 1 and Fig. 4 of the main text ($T_{m,i}$, $\Delta s_{m,i}(T)$ and $\Delta h_{m,i}(T)$ and $\Delta c_{p,i}$) have been derived from the fit to Eqs.5 as $s(\mathbf{x}) = \sqrt{(\mathrm{diag}[C(\mathbf{x})]}$, where $C(\mathbf{x})$ is the covariance matrix of the parameters vector including all errors of the fitted datasets.

All error bars in every quantity in the plots and tables show a confidence interval equal to 2σ centered at the mean, with σ the statistical error. For instance, $\Delta s_{\mathrm{GA/CT}} = -23.6(7)\mathrm{cal\,mol^{-1}K^{-1}}$ in Table 4 (main text) has $\sigma = 0.7\mathrm{cal\,mol^{-1}K^{-1}}$ meaning that the confidence interval goes from $-22.9\mathrm{cal\,mol^{-1}K^{-1}}$ to $-24.3\mathrm{cal\,mol^{-1}K^{-1}}$.

6 Fit of the NNBP parameters

The T-dependent NNBP entropies and enthalpies permit us to derive the heat capacity changes $\Delta c_{p,i}$ for each motif from the relations,

$$\Delta s_i = \Delta s_{m,i} + \Delta c_{p,i} \log(T/T_{m,i}) \tag{8a}$$

$$\Delta h_i = \Delta h_{m,i} + \Delta c_{p,i}(T - T_{m,i})\,, \tag{8b}$$

where $T_{m,i}$ is the melting temperature of motif i, and $\Delta s_{m,i}$ and $\Delta h_{m,i}$ are the entropy and enthalpy at $T = T_{m,i}$, respectively. The extraction of the NNBP thermodynamics parameters $(\Delta c_{p,i}, \Delta s_i, \Delta h_i, T_{m,i})$ has to be carried out carefully as the results are susceptible to experimental errors and parameters initialization. In particular, $\Delta s_{m,i}$, $\Delta h_{m,i}$, and $T_{r,i}$ strongly depend on their initialization values when directly fitted from Eqs.(8) as an error in $\Delta s_{m,i}$ ($\Delta h_{m,i}$) get compensated by $T_{m,i}$ and vice versa.

To derive the $\Delta c_{p,i}$, we fit the NNBP entropies to the equation $\Delta s_i(T) = A_i + \Delta c_{p,i} \log(T)$, being $A_i = \Delta s_{m,i} - \Delta c_{p,i} \log(T_{m,i})$. Notice that we derive $\Delta c_{p,i}$ from the NNBP entropies as they are obtained from the experimental

data, in contrast to enthalpies that are computed from the free energies. Given $\Delta c_{p,i}$, we fit the NNBP free energies, $\Delta g_i(T)$, to the equation

$$\begin{aligned}\Delta g_i(T) &= \Delta h_i(T) - T\Delta s_i(T) = \\ &= \Delta h_{m,i} + \Delta c_{p,i}(T - T_{m,i}) - T\left(\Delta s_{m,i} + \Delta c_{p,i}\log\left(\frac{T}{T_{m,i}}\right)\right) \\ &= B_i + \Delta c_{p,i}T - T\left(A_i + \Delta c_{p,i}\log\left(T\right)\right) .\end{aligned} \tag{9}$$

obtained by combining Eqs.(8) (blue dashed lines in Fig. 3B, main text). Notice that $B_i = \Delta h_{m,i} - \Delta c_{p,i}T_{m,i}$. By definition, $T_{m,i}$ is the high temperature value where $\Delta g_i(T_{m,i}) = 0$. Finally, a new fit to Eqs.(8a) and (8b) by using the previously derived values of $\Delta c_{p,i}$ and $T_{m,i}$ (red and blue dashed lines in Fig. 2D, main text), gives $\Delta s_{m,i}$ and $\Delta h_{m,i}$. The results are shown in Fig. 4 and Table 1 of the main text.

The statistical errors for $\Delta c_{p,i}$, $\Delta s_{m,i}$, $\Delta h_{m,i}$, and $T_{m,i}$ have been derived from the fits to Eqs.(8) and Eq.(9) as $s(\mathbf{x}) = \sqrt{(\mathrm{diag}[C(\mathbf{x})]}$, where $C(\mathbf{x})$ is the covariance matrix of the parameters vector (see Supplementary Methods, Sec. 5).

Supplementary References

[1] Rissone, P.: Thermodynamics and kinetics of nucleic acids folding (2023)

[2] Huguet, J.M., Ribezzi-Crivellari, M., Bizarro, C.V., Ritort, F.: Derivation of nearest-neighbor DNA parameters in magnesium from single molecule experiments. Nucleic Acids Res. **45**(22), 12921–12931 (2017)

[3] SantaLucia, J.: A unified view of polymer, dumbbell, and oligonucleotide DNA nearest-neighbor thermodynamics. Proc. Natl. Acad. Sci. U.S.A. **95**(4), 1460–1465 (1998)

[4] Owczarzy, R., Moreira, B.G., You, Y., Behlke, M.A., Walder, J.A.: Predicting stability of DNA duplexes in solutions containing magnesium and monovalent cations. Biochemistry **47**(19), 5336–5353 (2008)

[5] Severino, A., Monge, A.M., Rissone, P., Ritort, F.: Efficient methods for determining folding free energies in single-molecule pulling experiments. J. Stat. Mech.: Theory Exp **2019**(12), 124001 (2019)

[6] Forns, N., de Lorenzo, S., Manosas, M., Hayashi, K., Huguet, J.M., Ritort, F.: Improving signal/noise resolution in single-molecule experiments using molecular constructs with short handles. Biophys. J. **100**(7), 1765–1774 (2011)

[7] Robbins, H., Monro, S.: A stochastic approximation method. Ann. Math. Stat., 400–407 (1951)

[8] Curry, H.B.: The method of steepest descent for non-linear minimization problems. Q. Appl. Math. **2**(3), 258–261 (1944)

[9] Polyak, B.T.: Introduction to Optimization. Optimization Software vol. 1, p. 32 (1987)

[10] Qian, N.: On the momentum term in gradient descent learning algorithms. Neural Netw. **12**(1), 145–151 (1999)

[11] Bottou, L.: Large-scale machine learning with stochastic gradient descent. Proceedings of COMPSTAT'2010, 177–186 (2010)

[12] Bottou, L.: Stochastic gradient descent tricks. Neural networks: Tricks of the trade, 421–436 (2012)

[13] Nesterov, Y.: A method for unconstrained convex minimization problem with the rate of convergence o (1/kˆ 2). In: Doklady an Ussr, vol. 269, pp. 543–547 (1983)

[14] Achlioptas, P.: Stochastic Gradient Descent in Theory and Practice.

Stanford (2019)

[15] Woodside, M.T., Anthony, P.C., Behnke-Parks, W.M., Larizadeh, K., Herschlag, D., Block, S.M.: Direct measurement of the full, sequence-dependent folding landscape of a nucleic acid. Science **314**(5801), 1001–1004 (2006)

[16] Huguet, J.M., Bizarro, C.V., Forns, N., Smith, S.B., Bustamante, C., Ritort, F.: Single-molecule derivation of salt dependent base-pair free energies in DNA. Proc. Natl. Acad. Sci. U.S.A. **107**(35), 15431–15436 (2010)